PNAS RESEARCH ARTICLE | CELL BIOLOGY

RNA m^{1}A methylation regulates glycolysis of cancer cells through modulating ATP5D

Yingmin Wu[a,b,1], Zhuojia Chen[c,1], Guoyou Xie[a,1], Haisheng Zhang[a], Zhaotong Wang[a], Jiawang Zhou[a], Feng Chen[a], Jiexin Li[a], Likun Chen[c], Hongxin Niu[d], and Hongsheng Wang[a,2]

Edited by Kevin Struhl, Harvard Medical School, Boston, MA; received October 17, 2021; accepted May 5, 2022

Studies on biological functions of RNA modifications such as N^6-methyladenosine (m^{6}A) in mRNA have sprung up in recent years, while the roles of N^1-methyladenosine (m^{1}A) in cancer progression remain largely unknown. We find m^{1}A demethylase ALKBH3 can regulate the glycolysis of cancer cells via a demethylation activity dependent manner. Specifically, sequencing and functional studies confirm that ATP5D, one of the most important subunit of adenosine 5′-triphosphate synthase, is involved in m^{1}A demethylase ALKBH3-regulated glycolysis of cancer cells. The m^{1}A modified A71 at the exon 1 of ATP5D negatively regulates its translation elongation via increasing the binding with YTHDF1/eRF1 complex, which facilitates the release of message RNA (mRNA) from ribosome complex. m^{1}A also regulates mRNA stability of E2F1, which directly binds with ATP5D promoter to initiate its transcription. Targeted specific demethylation of ATP5D m^{1}A by dm^{1}ACRISPR system can significantly increase the expression of ATP5D and glycolysis of cancer cells. In vivo data confirm the roles of m^{1}A/ATP5D in tumor growth and cancer progression. Our study reveals a crosstalk of mRNA m^{1}A modification and cell metabolism, which expands the understanding of such interplays that are essential for cancer therapeutic application.

m^{1}A | metabolism | ATP5D | cancer cell

N^1-methyladenosine (m^{1}A) has been identified since the 1960s (1). As the predominant modification in transfer RNA (tRNA) and ribosome RNA (rRNA), the abundance of m^{1}A in message RNA (mRNA) is 10 times less common than that of N^6-methyladenosine (m^{6}A) (2, 3). In mRNA, m^{1}A has been discovered in every mRNA segment and acts as a unique type of base methylation to block Watson–Crick base pairing and alter mRNA structural stability (4, 5). TRMT6/TRMT61A complex in the cytosol and TRMT10C/TRMT61B complex in the mitochondria are putative m^{1}A methyltransferases (6). ALKBH3 has been identified as the only m^{1}A eraser which demethylates RNA (3, 7). Although it is prevalent, little is known about the functional roles in human diseases including cancer.

Recently, metabolic alteration is gaining increasing attention in cancer research due to the oncogenic roles to support malignant tumor initiation and progression (8). Cancer cells heavily rely on glycolysis to obtain energy even in the presence of oxygen (9), which is the most important feature of metabolic reprogramming in cancers. Blocking glycolysis has been considered as an attractive therapeutic intervention to suppress cancer cell growth and metastasis (10). Further, glycolysis can modulate tumor microenvironment to trigger the angiogenesis and immune evasion of cancers (11, 12). Therefore, understanding the molecular mechanisms regulating glycolysis is essential for investigating novel cancer therapy targets and strategies.

It has been revealed that interrelationship between metabolic reprogramming and epigenetic alterations can modulate each other to trigger cancer progression (13). For example, liver kinase B1 (LKB1) deficiency sensitizes cells and tumors to inhibition of serine biosynthesis and DNA methylation (14). Further, lactate-derived lactylation of histone lysine residues serves as an epigenetic modification that directly stimulates gene transcription from chromatin (15). As to RNA modification, the m^{6}A reader YTHDC2 can regulate of hepatic lipogenesis and triglyceride homeostasis (16), while R-2-hydroxyglutarate can attenuate aerobic glycolysis in leukemia by targeting the FTO/m^{6}A/PFKP/LDHB axis (17). Our recent study indicated that m^{6}A regulates glycolysis of cancer cells via methylation of 5′ untranslated region (5′UTR) of pyruvate dehydrogenase kinase 4 (PDK4) to regulate its translation elongation and mRNA stability (18). However, whether m^{1}A modification can regulate the metabolic programming of cancer cells and then modulate cancer development remains unknown.

Our present study reveals that m^{1}A can positively regulate glycolysis of cancer cells via regulation of ATP5D, a subunit of mitochondrial adenosine 5′-triphosphate (ATP)

Significance

The functions of N^1-methyladenosine (m^{1}A) in cancer development were largely unknown. We revealed m^{1}A can positively regulate the glycolysis of cancer cells via regulation of ATP5D. Specifically, m^{1}A regulates translation of ATP5D via YTHDF1/eRF3, and m^{1}A negatively regulated message RNA (mRNA) stability of E2F1, which initiates ATP5D transcription. Targeted specific demethylation of ATP5D m^{1}A by dm^{1}ACRISPR system can significantly increase the expression of ATP5D and glycolysis of cancer cells. Our study reveals a crosstalk of mRNA m^{1}A modification and cell metabolism, which broadens the multilayer regulation of metabolism and expands our understanding of such interplays that are essential for therapeutic application.

Author contributions: Z.C. and H.W. designed research; Y.W., G.X., H.Z., F.C., and J.L. performed research; Y.W., Z.C., G.X., Z.W., and J.Z. contributed new reagents/analytic tools; Y.W., Z.C., G.X., H.Z., Z.W., J.Z., F.C., J.L., L.C., H.N., and H.W. analyzed data; and H.W. wrote the paper.

The authors declare no competing interest.

This article is a PNAS Direct Submission.

[1]Y.W., Z.C., and G.X. contributed equally to this work.

[2]To whom correspondence may be addressed. Email: whongsh@mail.sysu.edu.cn.

This article contains supporting information online at http://www.pnas.org/lookup/suppl/doi:10.1073/pnas.2119038119/-/DCSupplemental.

Published July 8, 2022.

synthase which plays an important role in coupling proton translocation and ATP production (19). We found that m^1A methylation negatively regulates transcription and translation of ATP5D mRNA, which results in regulation of glycolysis and growth of cancer cells.

Results

m^1A Regulated Glycolysis and Malignancy of Cancer Cells. Since ALKBH3 has been identified as the only eraser for mRNA m^1A (3, 7), we generated ALKBH3$^{-/-}$ HeLa cells in our previous study (20) by using CRISPR/Cas9 editing system and SiHa stable knockdown (KD) cells by the use of short hairpin RNA (shRNA) (Fig. 1*A*). High-performance liquid chromatography-tandem mass spectrometry (HPLC-MS/MS) (Fig. 1*B*) and dot-blot (*SI Appendix*, Fig. S1*A*) analysis showed that levels of m^1A in mRNA of ALKBH3 KD cells were significantly greater than that in control cells. Knockdown of ALKBH3 suppressed growth (Fig. 1*C*), colonization (*SI Appendix*, Fig. S1*B*), migration (*SI Appendix*, Fig. S1*C*), and invasion (*SI Appendix*, Fig. S1*D*) of HeLa and SiHa cells while increased chemosensitivity of HeLa cells to doxorubicin (Dox) and cisplatin (CDDP) treatment (*SI Appendix*, Fig. S1*E*). Cells with knockdown of ALKBH3 exhibited significantly lower glucose consumption, lactate production rate, and ATP levels than that of their control cells (Fig. 1 *D*–*F*). Further, ALKBH3$^{-/-}$ HeLa (Fig. 1*F*) and sh-ALKBH3 SiHa (Fig. 1*G*) cells displayed decreased extracellular acidification rate (ECAR), which reflects overall glycolytic flux.

We then generated catalytically inactive ALKBH3 mutants R122S and L177A (20). The m^1A demethylation effect of ALKBH3 had been markedly decreased by mutation of R122S and L177A (*SI Appendix*, Fig. S1*F* and *G*). Further, neither R122S nor L177A mutants had comparable effect of wild-type (WT) ALKBH3-induced up-regulation of glucose consumption, lactate production, and ATP productions (Fig. 1 *I*–*K*). Overexpression of ALKBH3 WT constructs, while not R122S or L177A mutant, reversed the down-regulation of glucose consumption in ALKBH3$^{-/-}$ HeLa cells (Fig. 1*L*). It indicated that ALKBH3 can positively regulate cancer metabolism in an m^1A demethylase enzyme activity-dependent manner.

ATP5D Was Involved in m^1A-Regulated Glycolysis of Cancer Cells. We next investigated potential targets involved in m^1A-regulated metabolic shift of cancer cells. First, mRNA sequencing (mRNA-seq) showed in ALKBH3$^{-/-}$ cells, 667 genes were up-regulated while 252 genes were down-regulated (*SI Appendix*, Table S1). Gene Set Enrichment Analysis found that the epithelial mesenchymal transition (*SI Appendix*, Fig. S2*A*), angiogenesis (*SI Appendix*, Fig. S2*B*), and xenobiotic metabolism (*SI Appendix*, Fig. S2*C*) were also inhibited in ALKBH3$^{-/-}$ cells. Considering that there were different conclusions for m^1A sites in human transcriptome (2, 3, 5), we therefore evaluated whether the down-regulated genes were due to m^1A methylation by overlapping analysis these genes with the previously reported m^1A methylated mRNAs.

Overlap analysis showed that nine candidates overlapping among down-regulated genes in ALKBH3$^{-/-}$ HeLa cells and m^1A modified genes in three human cell lines including HeLa, HEK293T, and HepG2 identified by Dominissini et al. (2) (Fig. 2*A* and *SI Appendix*, Table S2). In addition, six overlapped genes were observed between down-regulated genes in ALKBH3$^{-/-}$ HeLa cells and m^1A modified genes in HEK293T identified by Li et al. (3) (Fig. 2*B* and *SI Appendix*, Table S2). Further, eight overlapped genes were observed between down-regulated genes in ALKBH3$^{-/-}$ cells and transcripts containing an m^1A-miCLIP cluster in HEK293T cells identified by Grozhik et al. (21) (Fig. 2*C* and *SI Appendix*, Table S2). Fifteen overlapped genes were observed between down-regulated genes in ALKBH3$^{-/-}$ cells and m^1A modified genes identified by Esteve-Puig et al. (22) (Fig. 2*D* and *SI Appendix*, Table S2). ATP5D was the only candidate gene simultaneously observed in four overlap analyses, while TRIM28 was simultaneously observed in three overlap analyses (Fig. 2*E*). Consistently, our m^1A-seq data revealed that there was significant enrichment of m^1A in coding sequence (CDS) regions of ATP5D in HeLa cells, further, this enrichment was further increased in ALKBH3$^{-/-}$ HeLa cells as compared with that in control (Fig. 2*F*), which is consistent with that in HEK293T identified by Li et al. (3) (*SI Appendix*, Fig. S2*D*). Knockdown of ALKBH3 can inhibit mRNA of ATP5D and TRIM28 in both HeLa and SiHa cells (*SI Appendix*, Fig. S2*E*), while the inhibition effect for ATP5D was greater than that for TRIM28.

ATP5D is the δ subunit of ATP synthase which plays an important role in coupling proton translocation and ATP production (19, 23). m^1A quantitative polymerase chain reaction (qPCR) confirmed that an approximately threefold m^1A antibody enriched ATP5D mRNA in HeLa cells, which was increased in ALKBH3$^{-/-}$ HeLa cells (Fig. 2*G*). Similar results were also obtained in SiHa cells (*SI Appendix*, Fig. S2*F*). However, neither m^1A pull down enrichment nor m^1A up-regulation in ALKBH3$^{-/-}$ HeLa cells were observed for the negative candidate gene *ATP5A1* (*SI Appendix*, Fig. S2*G*). It indicated that ATP5D mRNA was modified by m^1A and the methylation was regulated by ALKBH3.

ALKBH3 possesses the ability to demethylate m^1A and m^3C in RNA and single-stranded DNA (7), respectively. However, neither m^3C pull down enrichment nor m^3C up-regulation in ALKBH3$^{-/-}$ HeLa cells were observed for ATP5D mRNA (*SI Appendix*, Fig. S2*H*), which indicated that ALKBH3-regulated ATP5D should be m^1A-dependent rather than m^3C-dependent. Protein levels of ATP5D were decreased in ALKBH3 KD cells (Fig. 2*H*). Overexpression of ALKBH3, while not R122S or L177A, significantly increased protein expression of ATP5D (Fig. 2*I*). Consistently, overexpression of ALKBH3, while not ALKBH3-R122S or L177A, significantly suppressed the m^1A methylation of *ATP5D* mRNA in HeLa cells (Fig. 2*J*).

In order to confirm whether ATP5D was involved in m^1A-regulated glycolysis of cancer cells, both WT and ALKBH3$^{-/-}$ HeLa cells were transfected with ATP5D constructs (Fig. 2*K*). Overexpression of ATP5D can reverse the down-regulation of glucose consumption, lactate production rate, and ATP levels (Fig. 2*L*) and ECAR (Fig. 2*M*) of ALKBH3$^{-/-}$ HeLa cells. It confirmed that ATP5D is involved in m^1A-regulated glycolysis of cancer cells.

m^1A Negatively Regulated Transcription and Translation of ATP5D mRNA. We then investigated mechanisms responsible for m^1A-regulated expression of ATP5D. Quantitative real time–polymerase chain reaction (qRT-PCR) showed that the mature-mRNA (Fig. 3*A*) and precursor-mRNA (Fig. 3*B*) of ATP5D were decreased in ALKBH3 knockdown cells. There is no significant difference for stability of mature-mRNA (*SI Appendix*, Fig. S3*A*) or splicing rate of precursor-mRNA (*SI Appendix*, Fig. S3*B*) of ATP5D between WT and ALKBH3$^{-/-}$ cells. Further, by separating nuclear and cytoplasmic RNAs (*SI Appendix*, Fig. S3*C*), we found that there was no difference for subcellular localization of neither mRNA (*SI Appendix*, Fig. S3*D*) nor protein (*SI Appendix*, Fig. S3*C*) of ATP5D between WT and ALKBH3$^{-/-}$ HeLa cells.

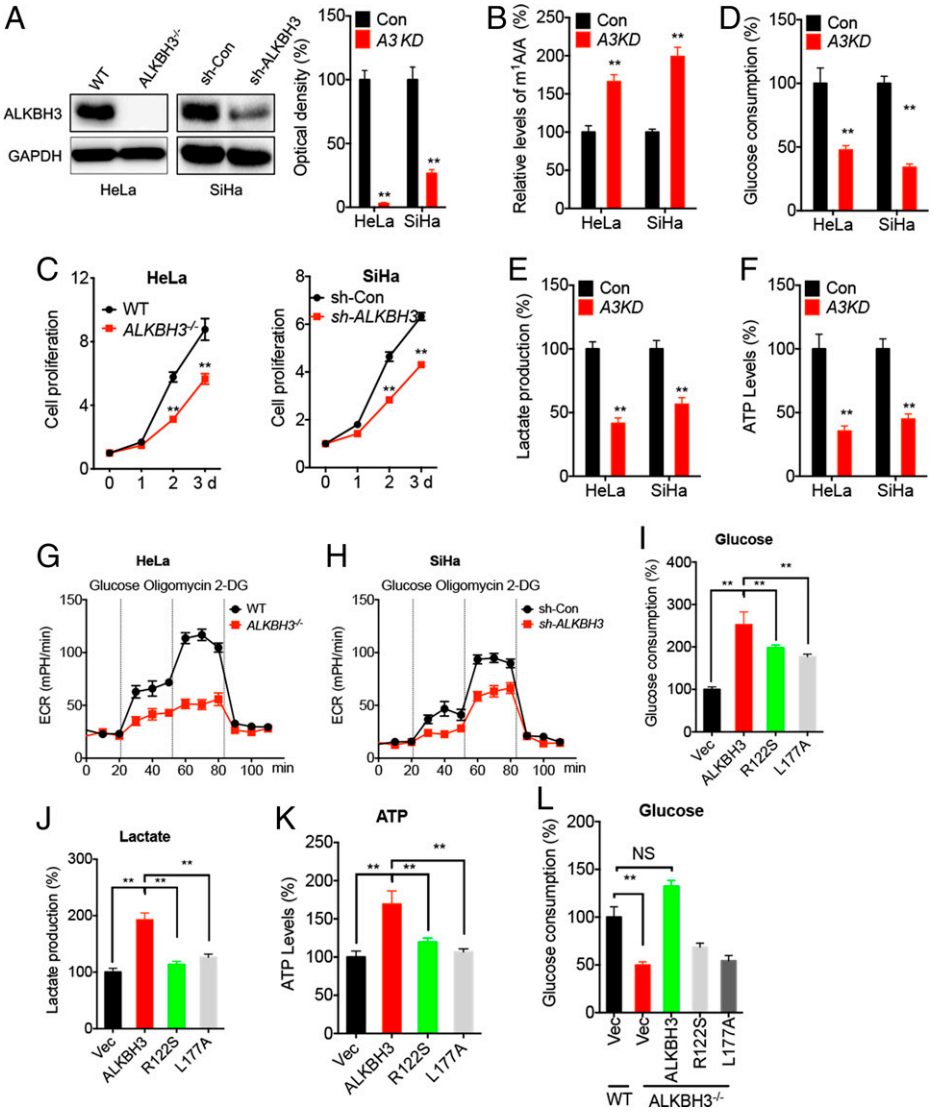

Fig. 1. m^{1}A regulated glycolysis and malignancy of cancer cells. (*A–C*) The expression of ALKBH3 (*A*), m^{1}A/A ratio of mRNA (*B*), and relative fold of cell proliferation (*C*) of ALKBH3$^{-/-}$ HeLa, sh-ALKBH3 SiHa and control cells. (*D–F*) The glucose consumption (*D*), lactate production (*E*), and ATP levels (*F*) in ALKBH3$^{-/-}$ HeLa, sh-ALKBH3 SiHa, and control cells; (*G* and *H*) The cellular ECAR of ALKBH3$^{-/-}$ HeLa (*G*) or sh-ALKBH3 SiHa (*H*) cells and control cells. (*I–K*) The glucose consumption (*I*), lactate production (*J*), and ATP (*K*) levels in HeLa cells transfected with vector control, ALKBH3, ALKBH3-R122S, or ALKBH3-L177A constructs for 48 h. (*L*) WT and ALKBH3$^{-/-}$ HeLa cells were transfected with vector control, ALKBH3, ALKBH3-R122S, or ALKBH3-L177A constructs for 48 h, the glucose consumption was checked.

However, deletion of ALKBH3 can significantly decrease the promoter activities of ATP5D (Fig. 3*C*). However, no similar effect has been observed for pyruvate dehydrogenase kinase 4 (PDK4), one target found to be regulated by m^{6}A in our previous study (18) while not observed in m^{1}A induced variated genes in the present study (Fig. 3*C*). Further, nuclear run-on reverse transcription PCR (RT-qPCR) assay showed that the nascent transcript of ATP5D in ALKBH3 KD cells were significantly less than that in control cells (Fig. 3*D*). Consistently, WT ALKBH3, while not ALKBH3 mutants R122S and L177A, can increase the promoter activities of ATP5D in HeLa cells (Fig. 3*E*). It suggested that m^{1}A can negatively regulate transcription of ATP5D.

We further investigated the potential effect of m^{1}A on translation and posttranslation of ATP5D. The half-lives of ATP5D protein were similar between WT and ALKBH3$^{-/-}$ HeLa cells (Fig. 3*F*). Further, co-immunoprecipitation (co-IP) analysis showed that there is no direct protein–protein interaction between endogenous ALKBH3 and ATP5D (*SI Appendix*, Fig. S3*E*). However, knockdown of ALKBH3 significantly decreased the translation efficiency of endogenous *ATP5D* mRNA (24) (Fig. 3*G*). Consistently, WT ALKBH3, while not R122S and L177A mutants, can increase the mRNA (Fig. 3*H*) and translation efficiency (Fig. 3*I*) of ATP5D in HeLa cells. We further generated luciferase reporters by fusion of F-Luc and *ATP5D* CDS regions in pmiR-GLO plasmid (Fig. 3*J*). The dual-luciferase assay showed that translation efficiency of ATP5D in ALKBH3$^{-/-}$ HeLa cells was significantly less than that in HeLa WT cells (Fig. 3*J*). It suggested that m^{1}A can negatively control ATP5D translation.

We further checked mechanisms involved in m^{1}A-regulated translation of ATP5D. After performing ribosome profile, we isolated nontranslating fraction (<40S), translation initiation fraction (including 40S and 60S ribosomes, 80S monosomes, <80S) and translation active polysomes (>80S) (Fig. 3*K*). qPCR showed *ATP5D mRNA* in translation active polysomes (>80S), rather than that in monosome, of ALKBH3$^{-/-}$ cells were significantly lower than that in WT cells (Fig. 3*L*). Read coverage plots of the Ribo sequencing (Ribo-seq) and RNA sequencing (RNA-seq) data for ATP5D showed a dramatic decrease in ribosome occupancy in ALKBH3$^{-/-}$ cells (Fig. 3*M*). It indicated that ALKBH3 and m^{1}A regulated the translation elongation and/or termination of ATP5D.

YTHDF1/eRF1 Was Involved in m^{1}A-Regulated Translation of ATP5D mRNA. YTHDF1/2/3 and YTHDC1 can recognize m^{1}A methylated mRNA to regulate translation (25–27). CLIP-PCR showed that YTHDF1/2/3 and YTHDC1 can bind with ATP5DmRNA, while only the binding with YTHDF1 was

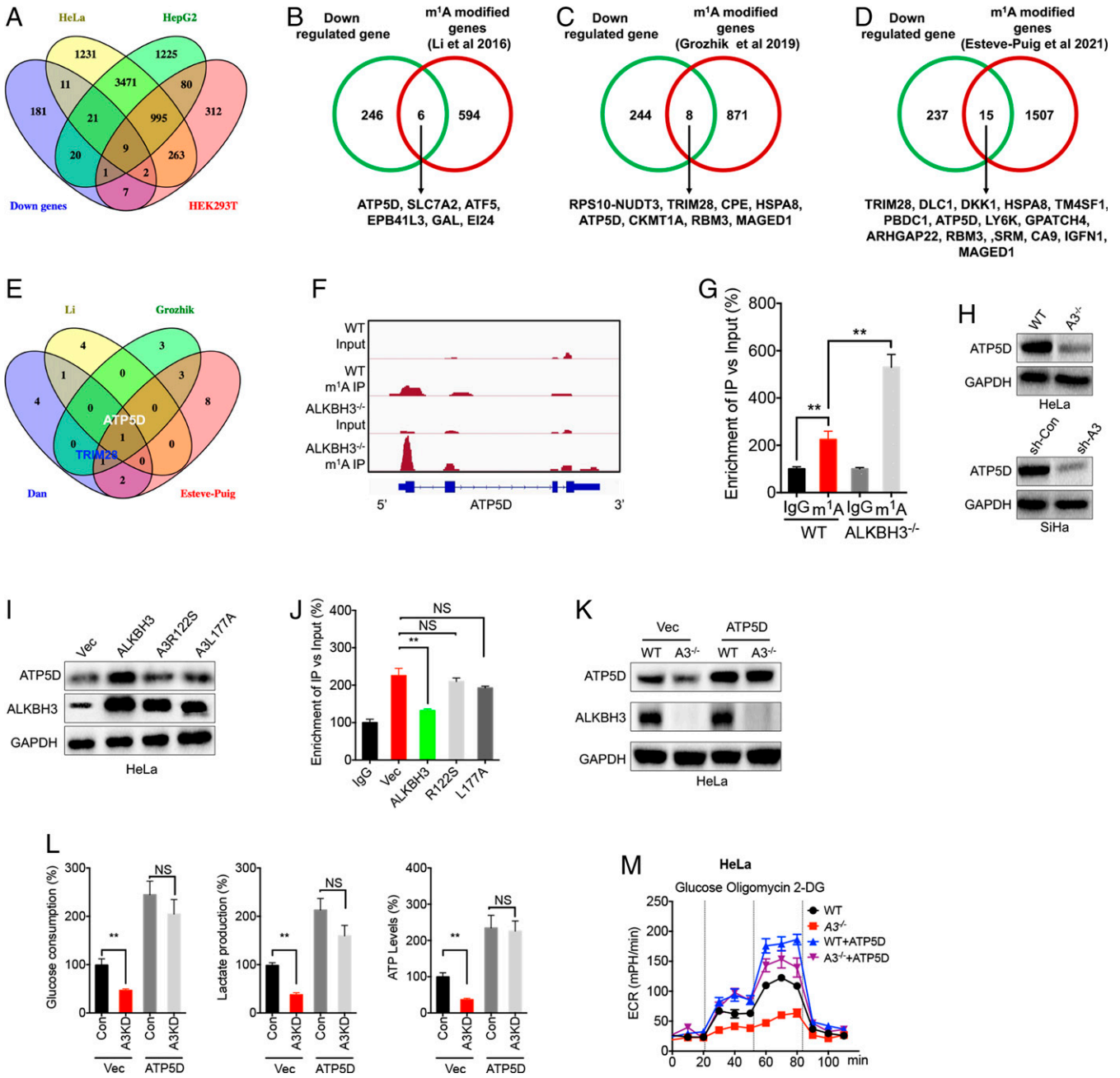

Fig. 2. ATP5 was involved in m^{1}A-regulated glycolysis of cancer cells. (*A*) Venn diagram shows substantial and significant overlap among down-regulated genes in ALKBH3$^{-/-}$ HeLa cells, and m^{1}A enriched genes in HeLa, HEK293T, and HepG2 cells (2). (*B–D*) Venn diagram shows substantial and significant overlap among down-regulated genes in ALKBH3$^{-/-}$ HeLa cells, and (*B*) m^{1}A enriched genes in HEK293T identified by Li et al. (3), (*C*) transcripts containing an m^{1}A-miCLIP cluster in HEK293T cells identified by Grozhik et al. (21), and (*D*) m^{1}A modified genes identified by Esteve-Puig et al. (22). (*E*) Venn diagram shows mRNAs overlap among the analysis of (*A*)–(*D*). (*F*) m^{1}A peaks were enriched in CDS of *ATP5D* genes from m^{1}A RIP-seq in WT or ALKBH3$^{-/-}$ HeLa cells. (*G*) m^{1}A RIP-qPCR analysis of ATP5D mRNA in WT and ALKBH3$^{-/-}$ HeLa cells. (*H*) The protein expression of ATP5D was measured in ALKBH3$^{-/-}$ HeLa or sh-ALKBH3 SiHa cells and control cells. (*I* and *J*) The expression (*I*) and m^{1}A enrichment (*J*) of ATP5D in HeLa cells transfected with vector control (pcDNA), ALKBH3, ALKBH3-R122S, or ALKBH3-L177A constructs for 24 h. (*K* and *L*) WT or ALKBH3$^{-/-}$ HeLa cells transfected with ATP5D constructs or vector control for 24 h (*K*) and then the glucose consumption, lactate production, and ATP levels were checked (*L*). (*M*) The cellular ECAR in WT or ALKBH3$^{-/-}$ HeLa cells transfected with ATP5D constructs or vector control for 24 h.

significantly increased in ALKBH3$^{-/-}$ cells (Fig. 4*A*). Consistently, increased binding between YTHDF1 and ATP5D mRNA in sh-ALKBH3 SiHa cells have been observed by CLIP-qPCR (Fig. 4*B*). It indicated that YTHDF1 may be involved in m^{1}A-regulated expression of ATP5D.

Subsequently, we checked the binding between ATP5D mRNA with the key factors for translation initiation, elongation, and termination. Results showed binding between ATP5D and translation initiation factor eIF4E was not variated in ALKBH3$^{-/-}$ cells (*SI Appendix*, Fig. S4*A*). Further, the binding between ATP5D mRNA with two elongation factors eEF-2 or eEF-1 in ALKBH3$^{-/-}$ cells was not significantly variated (*SI Appendix*, Fig. S4*B*). We further evaluated the binding between ATP5D mRNA with eukaryotic termination factors eRF1 and eRF3 (28). The binding of ATP5D mRNA with release factors eRF1, while not eRF3, was significantly increased in ALKBH3$^{-/-}$ HeLa (Fig. 4*C*) and sh-ALKBH3 SiHa (Fig. 4*D*) cells. It indicated that knockdown of ALKBH3 can increase the binding between ATP5D mRNA and eRF1, which resulted in enhanced termination efficiency.

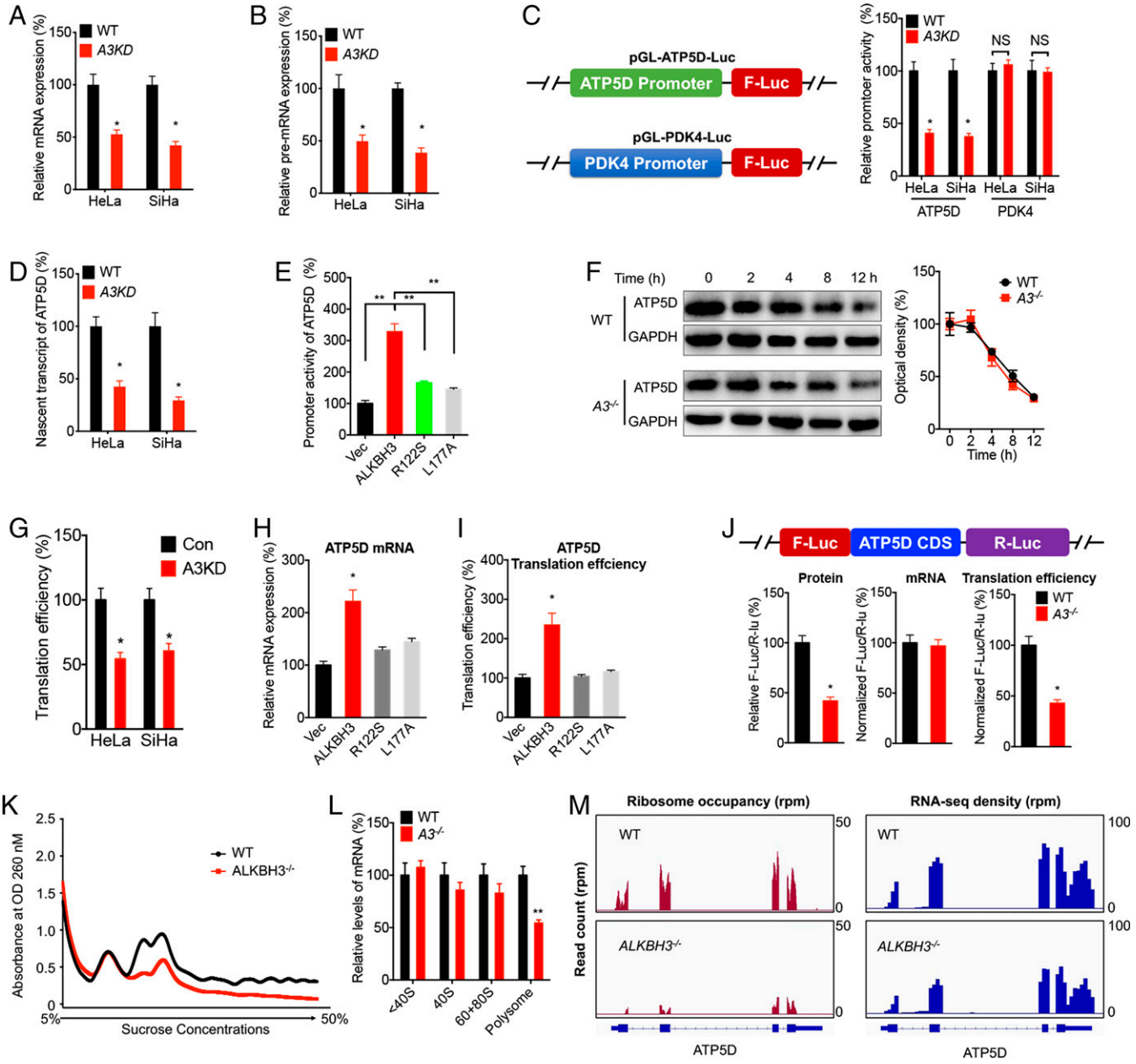

Fig. 3. m^{1}A negatively regulated transcription and translation of ATP5D mRNA. (*A* and *B*) The mature mRNA (*A*) and precursor mRNA (*B*) of ATP5D in ALKBH3$^{-/-}$ HeLa, sh-ALKBH3 SiHa, and control cells. (*C*) The promoter activities of ATP5D and PDK4 in ALKBH3$^{-/-}$ HeLa, sh-ALKBH3 SiHa, and control cells. (*D*) The nascent transcript of ATP5D in ALKBH3$^{-/-}$ HeLa, sh-ALKBH3 SiHa, and control cells checked by nuclear run-on assay. (*E*) The promoter activities of ATP5D in HeLa cells cotransfected with promoter reporter and WT or mutant ALKBH3 constructs for 24 h. (*F*) WT or ALKBH3$^{-/-}$ HeLa cells were treated with CHX for 0–12 h, the protein expression of ATP5D was detected (*Left*) and quantitatively analyzed (*Right*). (*G*) The translation efficiency of endogenous ATP5D was checked by normalization of ATP5D protein levels to the relative mRNA abundance. (*H*) HeLa cells were transfected with vector control, WT, and mutant ALKBH3 for 24 h, the mRNA of ATP5D was checked. (*I*) The translation efficiency of ATP5D in HeLa cells transfected with vector control, WT, and mutant ALKBH3 for 24 h. (*J*) HeLa cells were transfected with pmirGLO-ATP5D reporter for 24 h. Levels of F-Luc/R-Luc, mRNA of F-Luc/R-Luc, and the relative translation efficiency of F-Luc were checked. The translation efficiency is defined as the quotient of F-Luc/R-Luc divided by mRNA abundance. (*K*) The polysome profiling of WT or *Alkbh3*$^{-/-}$ HeLa cells were analyzed. (*L*) Analysis of ATP5D mRNA in <40S, 40S, 60S+80S, and polysome in WT and ALKBH3$^{-/-}$ HeLa cells by qRT-PCR. (*M*) BedGraphs of total mRNA levels (RNA-seq) and RPFs (Ribo-seq) for the ATP5D genes in WT and ALKBH3$^{-/-}$ HeLa cells.

RNA modification readers can interact with translation regulators to modulate translation efficiency (29). Co-IP analysis showed that YTHDF1 and eRF1, while not eEF-1/-2 or eRF3, was significantly increased in ALKBH3$^{-/-}$ HeLa (Fig. 4*E*) and sh-ALKBH3 SiHa (Fig. 4*F*) cells. The binding between YTHDF1 and eRF1 was RNA-dependent since RNase treatment can decrease this binding (Fig. 4*G*). We constructed ATP5D overexpression plasmid with 2 × MS2bs and performed co-IP analysis by HA antibody (Fig. 4*H*). YTHDF1/eRF1 was more abundant in *ATP5D* mRNA in ALKBH3$^{-/-}$ cells compared to control (Fig. 4*I*). Knockdown of YTHDF1 attenuated ALKBH3-induced protein expression of ATP5D (Fig. 4*J*), while it had no significant effect on ALKBH3 mRNA (Fig. 4*K*). It suggested that YTHDF1 may recognize m1A methylated ATP5D mRNA and recruit eRF1 to suppress translation elongation and enhance termination efficiency.

A71 at Exon 1 was the Key Site of m^{1}A Methylation and Translation of ATP5D. We further investigated the methylation site of ATP5D. m^{1}A-RIP-PCR showed that the m^{1}A enrichment of *ATP5D* CDS, rather than 5′UTR or 3′UTR, was significantly increased in ALKBH3$^{-/-}$ cells (Fig. 5*A*), suggesting

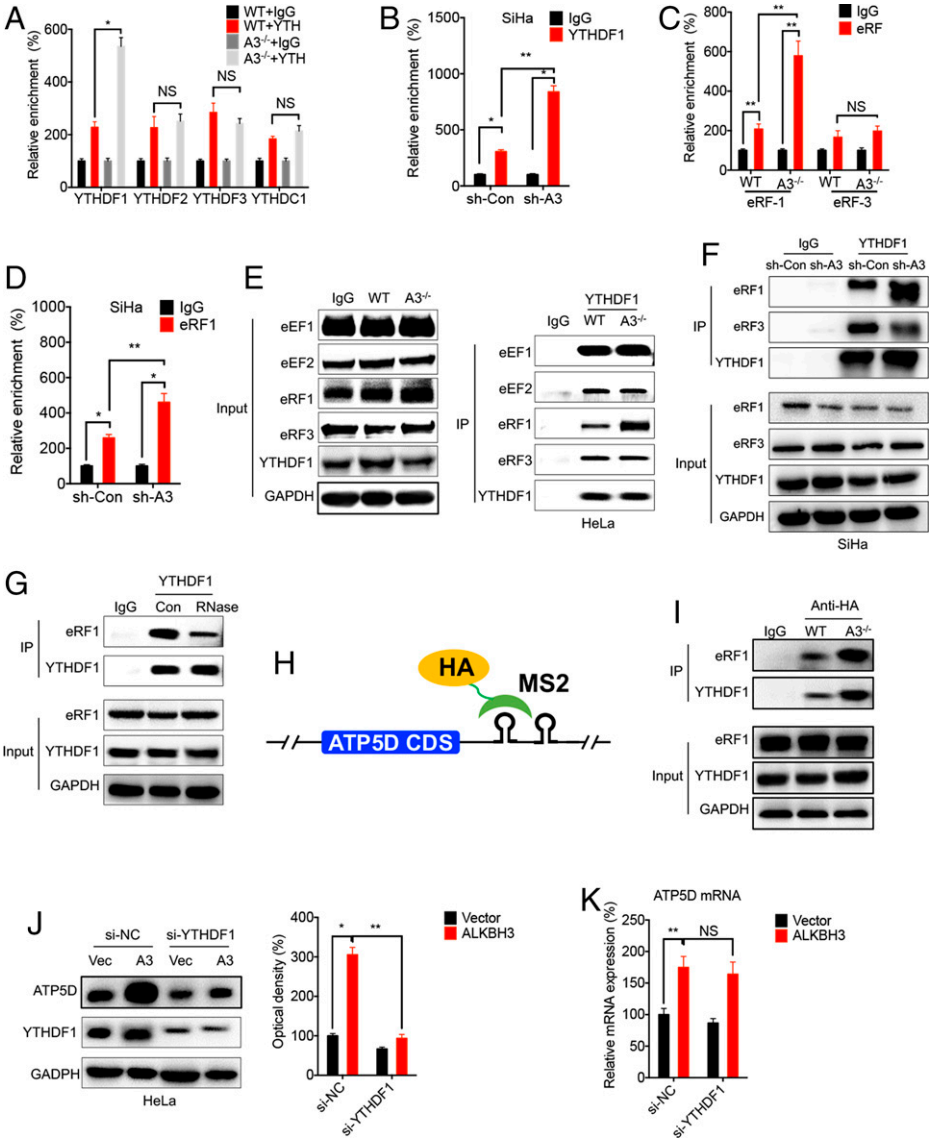

Fig. 4. YTHDF1/eRF1 was involved in m^{1}A-regulated translation of ATP5D mRNA. (*A*) CLIP-qPCR analysis of *ATP5D* mRNA in WT and ALKBH3$^{-/-}$ HeLa cells by use of antibodies of YTHDF1/2/3 or YTHDC1. (*B*) CLIP-qPCR analysis of *ATP5D* mRNA in sh-control and sh-ALKBH3 Siha cells by use of antibody of YTHDF1. (*C*) CLIP-qPCR analysis of *ATP5D* mRNA in WT and ALKBH3$^{-/-}$ HeLa cells by use of antibody of eRF1 or eRF3. (*D*) CLIP-qPCR analysis of *ATP5D* mRNA in sh-control and sh-ALKBH3 Siha cells by use of antibody of eRF1. (*E*) Binding between YTHDF1 with eEF-1/2 or eRF1/3 was checked by immunoprecipitation by pull-down of YTHDF1. (*F*) Binding between YTHDF1 with eRF1/3 in sh-ALKBH3 SiHa and control cells were checked by immunoprecipitation by pull down of YTHDF1. (*G*) Cell lysis of HeLa cells were treated with or without RNase, and the binding between YTHDF1 with eRF1 was checked by immunoprecipitation. (*H* and *I*) Interactions between *ATP5D* mRNA (β-MS2bs) and YTHDF1/eRF1 in WT and ALKBH3$^{-/-}$ HeLa cells were checked by immunoprecipitation by pull-down with pulled recombinant HA-MS2 protein. (*J* and *K*) HeLa cells were cotransfected with si-NC, si-YTHDF1, vector control, and ALKBH3 plasmid for 24 h, and the protein (*J*) and mRNA (*K*) expression of ATP5D were checked.

that m^{1}A methylation in CDS. Further, fragmented RNA m^{1}A-RIP-PCR showed enrichment of exon 1, rather than exon 2, 3, or 4, was significantly increased in ALKBH3$^{-/-}$ cells (Fig. 5*B*). Further, overexpression of ALKBH3 can decrease the m^{1}A methylation of ATP5D exon 1 (*SI Appendix*, Fig. S5*A*), while had no similar effect on ATP5D exon 2 (*SI Appendix*, Fig. S5*B*), in HeLa cells. It suggested that the m^{1}A methylation occurs at the exon 1 of ATP5D mRNA.

There are 12 "A" sites in the exon 1 (*SI Appendix*, Fig. S5*C*). Considering that m^{1}A methylation may occur in highly structured or GC-rich regions, we mutated seven "A" sites in the GC-rich regions to generate pmiR-GLO-exon1-WT and exon1-Mut-1/2/3/4 (Fig. 5*C*). Mutation of A71, while not others, can significantly increase the expression of F-Luc in HeLa cells (Fig. 5*D*). Deletion of ALKBH3-suppressed expression of F-Luc/R-Luc was significantly reversed by the mutation of A71, while not others (Fig. 5*D*). Over expression of ALKBH3 can significantly increase the expression of F-Luc of pmiR-GLO-exon1-WT, while this effect was markedly attenuated as for pmiR-GLO-exon1-Mut2 (A71 mutation) (Fig. 5*E*). Further, deletion of ALKBH3 can significantly increase the m^{1}A methylation of F-Luc-ALKBH3-exon1 fusion mRNA, however, the A71 mutation can decrease the m^{1}A methylation of fusion mRNA and further block ALKBH3 deletion-increased m^{1}A of fusion mRNA (Fig. 5*F*). We further performed m^{1}A-induced reverse transcription (RT) arrest in the ATP5D mRNA using the primer extension assay. RT was arrested at m^{1}A-71, but not at A53 or A105 (Fig. 5*G*), indicating m^{1}A-71 is a true methylation residue (6, 30).

A single-base elongation- and ligation-based qPCR amplification method (termed "SELECT") was developed according to the previous study (31) to confirm the site (Fig. 5*H*). The results of SELECT confirmed the m^{1}A site in the Exon1 region of ATP5D at A71 in both HeLa and SiHa cells (Fig. 5*I*), while the nearby nucleotide A65 showed no m^{1}A modification (*SI Appendix*, Fig. S5*D*). Our data confirmed that the m^{1}A at A71 of the ATP5D exon 1 exists and is reversibly modified.

In addition, deletion of ALKBH3 had no significant effect on the mRNA expression of Flag-fused WT and A71C mutant ATP5D mRNA (Fig. 5*J*), however, the deletion of ALKBH3-suppressed protein expression of ATP5D was abolished by A71C mutant (Fig. 5*K*). Consistently, A71C mutant abolished the down-regulation of translation efficiency of ATP5D in ALKBH3$^{-/-}$ cells (Fig. 5*L*). It might be due to the mutation of A71 to C has a great influence on the secondary structure of ATP5D mRNA (*SI Appendix*, Fig. S5*F*). Similarly, the

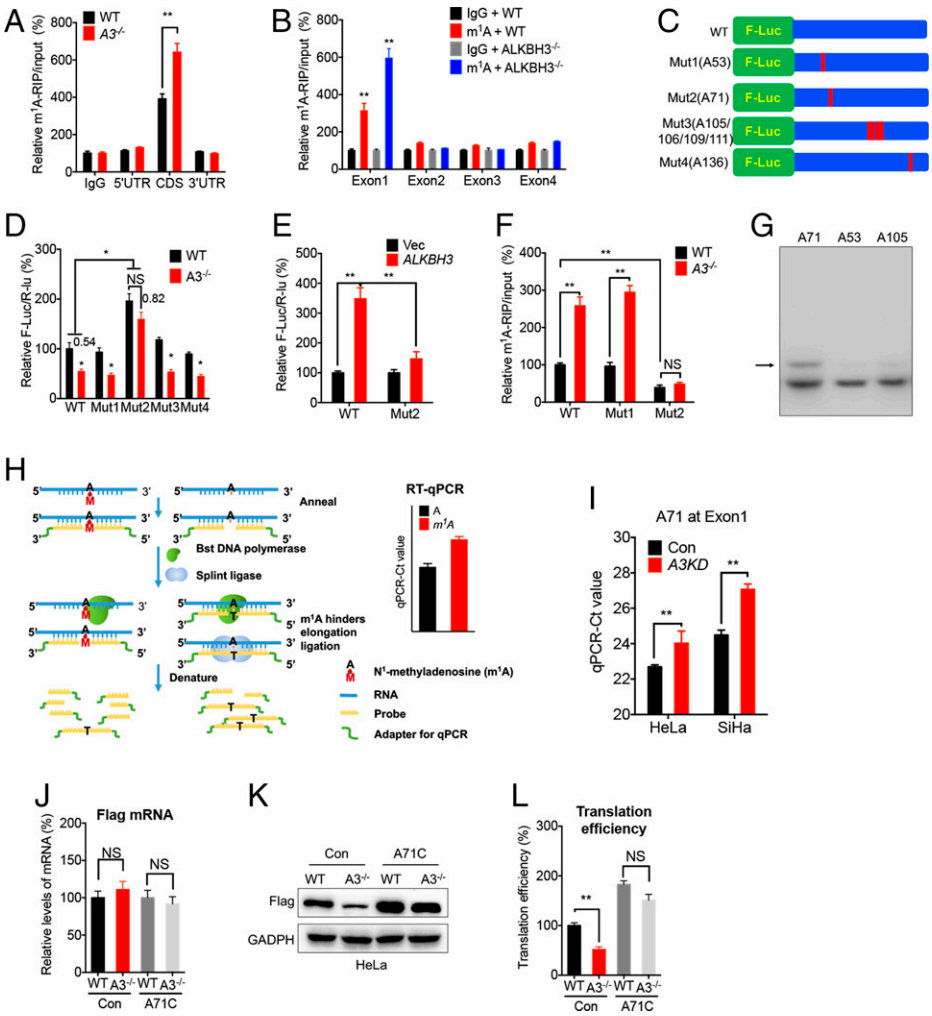

Fig. 5. A71 at exon 1 was the key site of m^{1}A methylation of ATP5D. (*A*) The m^{1}A in ATP5D in WT and ALKBH3$^{-/-}$ HeLa cells were analyzed by m^{1}A-RIP-qPCR using fragmented RNA. (*B*) The m^{1}A in ATP5D in WT and ALKBH3$^{-/-}$ HeLa cells was analyzed by m^{1}A-RIP-qPCR using fragmented RNA to analyze the m^{1}A enrichment of different exons. (*C*) Schematic representation of mutated (*A*)–(*C*) exon 1 of ATP5D mRNA of pmirGLO vector to investigate the roles of m^{1}A in ATP5D expression. (*D*) The relative luciferase activity of F-Luc/R-Luc of pmirGLO-exon1-WT, or pmirGLO-exon1-Mut-1/-2/-3/-4 in WT and ALKBH3$^{-/-}$ HeLa cells. (*E*) The relative luciferase activity of F-Luc/R-Luc of pmirGLO-exon1-WT, or pmirGLO-exon1-Mut-2 in HeLa cells cotransfected with vector control or ALKBH3 constructs. (*F*) WT and ALKBH3$^{-/-}$ HeLa cells were transfected with pmirGLO-exon1-WT or pmirGLO-exon1-Mut-1/-2 for 24 h, and the m^{1}A in F-Luc-exon fusion mRNA were analyzed by m^{1}A-RIP-qPCR. (*G*) The RNA primer extension shows that the A−71 is m^{1}A methylated. Purified mRNA from HeLa cells is immunoprecipitated by m^{1}A antibody. (*H*) Illustration of the SELECT m^{1}A detection method for specific transcripts. (*I*) The threshold cycle (CT) of qPCR showing SELECT results for detecting m^{1}A site in ATP5D at A71 in ALKBH3$^{-/-}$ HeLa or sh-ALKBH3 SiHa cells and control cells. (*J*–*L*) WT and ALKBH3$^{-/-}$ HeLa cells were transfected with constructs of Flag-ATP5D-WT and Flag-ATP5D-A71C for 24 h, and the mRNA (*J*), protein (*K*), and translation efficiency (*L*) were checked.

∼5 kcal/mol destabilization of m^{1}A on RNA duplex may markedly alter the secondary structure of ATP5D mRNA. All these data suggested that A71 of ATP5D was the site for m^{1}A methylation-regulated translation.

E2F1 Was Involved in ALKBH3-Regulated Transcription of ATP5D. The ENCODE chromatin immunoprecipitation sequencing (ChIP-seq) data in ChIPBase (32), PROMO with 5% maximum matrix dissimilarity rate (33), and JASPAR (34) were used to identify transcription factors (TFs) involved in m^{1}A regulated transcription of ATP5D. Among the identified factors (*SI Appendix*, Table S3), six factors including MZF1, CEBPB, YY1, CEBPA, E2F1, and GATA2 were overlapping among three databases (Fig. 6*A*). Among the six identified factors, mRNA expression of E2F1 decreased in ALKBH3 knockdown HeLa (Fig. 6*B*) and SiHa (*SI Appendix*, Fig. S6*A*) cancer cells. Further, ALKBH3 knockdown decreased the protein expression of E2F1 in cancer cells (Fig. 6*C*). Consistently, overexpression of ALKBH3 increased the mRNA (*SI Appendix*, Fig. S6*B*) and protein (*SI Appendix*, Fig. S6*C*) expression of E2F1.

Overexpression of E2F1 (*SI Appendix*, Fig. S6*D*) increased the precursor mRNA (Fig. 6*D*) and promoter activity (Fig. 6*E*) of ATP5D. In addition, overexpression of E2F1 attenuated deletion of ALKBH3-induced down-regulation of ATP5D mature mRNA (Fig. 6*F*) and protein (Fig. 6*G*). E2F1 can restore deletion of ALKBH3-suppressed transcriptional activities of ATP5D (Fig. 6*H*). ChIP-qPCR assays demonstrated that E2F1 had a significant enrichment of ATP5D promoter over normal immunoglobulin G (IgG) control (Fig. 6*I*), indicating a direct binding between E2F1 and ATP5D promoter. The prediction results by JASPAR indicated two putative sites with 85% similarity in sequence of E2F1 binding motif (Fig. 6*J*). ChIP-qPCR assays demonstrated the binding of E2F1 with putative site 1 was much greater than that with putative site 2 in HeLa cells (Fig. 6*K*). We then mutant the two putative sites of ATP5D promoter to generate pGL3-ATP5D-Mut 1 and pGL3-ATP5D-Mut 2 reporter (*SI Appendix*, Fig. S6*E*). Results showed that mutate of site 1, while not site 2, can significantly abolish E2F1-induced expression of F-Luc in HeLa cells (Fig. 6*L*). It suggested that E2F1, which was regulated by ALKBH3, can regulate the

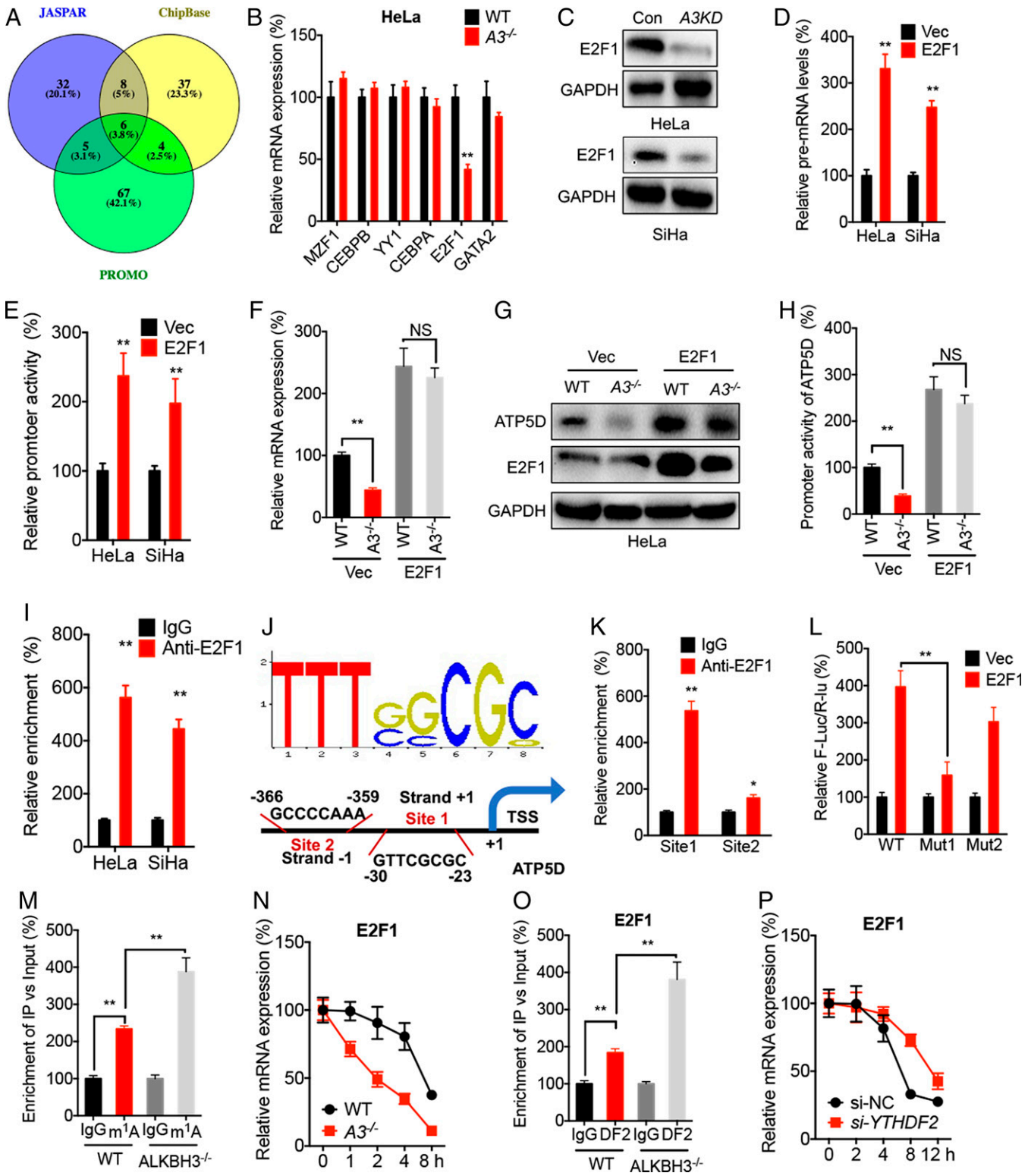

Fig. 6. E2F1 was responsible for m^{1}A-regulated transcription of ATP5D. (*A*) Venn diagram shows the overlap of transcription factors of ATP5D predicted by PROMO ChIPBase, and JASPAR. (*B*) The mRNA levels of predicted TFs in WT and ALKBH3$^{-/-}$ HeLa cells were checked by qRT-PCR. (*C*) The expression of E2F1 was checked by Western blot analysis. (*D*) Cells were transfected with vector control or E2F1 constructs for 24 h, and the precursor mRNA levels of ATP5D were checked by qRT-PCR. (*E*) Cells were cotransfected with ATP5D promoter luciferase reporter (pGL-ATP5D) with vector control or E2F1 constructs for 24 h, and the promoter activity was checked. (*F* and *G*) WT and ALKBH3$^{-/-}$ HeLa cells were transfected with vector control or E2F1 constructs for 24 h, and the mRNA (*F*) and protein (*G*) levels of ATP5D were checked. (*H*) WT and ALKBH3$^{-/-}$ HeLa cells were transfected with ATP5D promoter luciferase reporter (pGL-ATP5D) with vector control or E2F1 constructs for 24 h, and the promoter activity was checked. (*I*) The binding between ATP5D promoter and E2F1 was checked by ChIP-PCR by use of anti-E2F1 antibody. (*J*) Two putative sites with 85% similarity in sequence of E2F1 binding motif in promoter of ATP5D. (*K*) The binding between ATP5D promoter two putative sites and E2F1 in HeLa cells was checked by ChIP-PCR by use of anti-E2F1 antibody. (*L*) The WT and two mutant ATP5D promoter luciferase reporter (pGL-ATP5D) in HeLa cells transfected with vector control or E2F1 constructs. (*M*) m^{1}A RIP-qPCR analysis of E2F1 mRNA in WT and ALKBH3$^{-/-}$ HeLa cells. (*N*) WT and ALKBH3$^{-/-}$ HeLa cells were treated with Act-D for 0–8 h, and the mRNA stability of E2F1 was checked by qRT-PCR. (*O*) CLIP-qPCR analysis of *E2F1* mRNA in WT and ALKBH3$^{-/-}$ HeLa cells by use of antibodies of YTHDF2. (*P*) HeLa cells were pretransfected with si-NC or si-YTHDF2 for 24 h and then further treated Act-D for 0–8 h. The mRNA stability of E2F1 was checked by qRT-PCR.

transcription of ATP5D via binding with the putative site at -30 to -23 of ATP5D promoter.

Previous studies suggested that E2F1 mRNA was modified by m^{1}A methylation in human cells including HeLa (2), HepG2 (2), and HEK293T cells (3). We found an approximate twofold m^{1}A antibody enriched E2F1 mRNA in HeLa cells, while this enrichment was significantly increased in ALKBH3$^{-/-}$ HeLa cells (Fig. 6*M*). Further, knockdown of ALKBH3 decreased mRNA stability of E2F1 (Fig. 6*N*), while it had no effect on its expression of precursor mRNA (*SI Appendix*, Fig. S6*F*) or protein stability (*SI Appendix*, Fig. S6*G*). Increasing m^{1}A levels can destabilize known m^{1}A-containing RNAs (27), likely through YTHDF2-mediated mRNA decay (35). The binding between YTHDF2 and E2F1 mRNA in ALKBH3$^{-/-}$ cells were greater than that in WT cells (Fig. 6*O*). Consistently, si-YTHDF2 can increase the mRNA stability of E2F1 (Fig. 6*P*). All these data suggested that E2F1 was involved in ALKBH3-regulated transcription of ATP5D.

Targeting m^{1}A of ATP5D by dm^{1}ACRISPR to Regulate Glycolysis. To specific demethylate m^{1}A of ATP5D mRNA, we developed the dm^{1}ACRISPR by fusing the catalytically dead type VI-B Cas13 enzyme with the m^{1}A demethylase ALKBH3 according to our previous study (36) (Fig. 7*A* and *SI Appendix*, Fig. S7*A*) and designed three guide RNAs (gRNAs) to target the mRNA of ATP5D (Fig. 7*B*). WT Cas13b cotransfected with three gRNAs, respectively, can significantly decrease the mRNA levels of ATP5D (*SI Appendix*, Fig. S7*B*). However, transfection with gRNA alone (*SI Appendix*, Fig. S7*C*) or gRNA with dCas13b (*SI Appendix*, Fig. S7*D*) had no significant effect on the mRNA expression of ATP5D in HeLa cells.

SELECT-qPCR (Fig. 7*C*) and m^{1}A-RIP-qPCR (Fig. 7*D*) showed that m^{1}A levels of targeted site on ATP5D mRNA were significantly decreased after transfecting cells with gRNAs, and dCas13b-ALKBH3 in HeLa cells with gRNA-1 had the strongest demethylation effect. Results showed that dm^{1}ACRISPR targeting

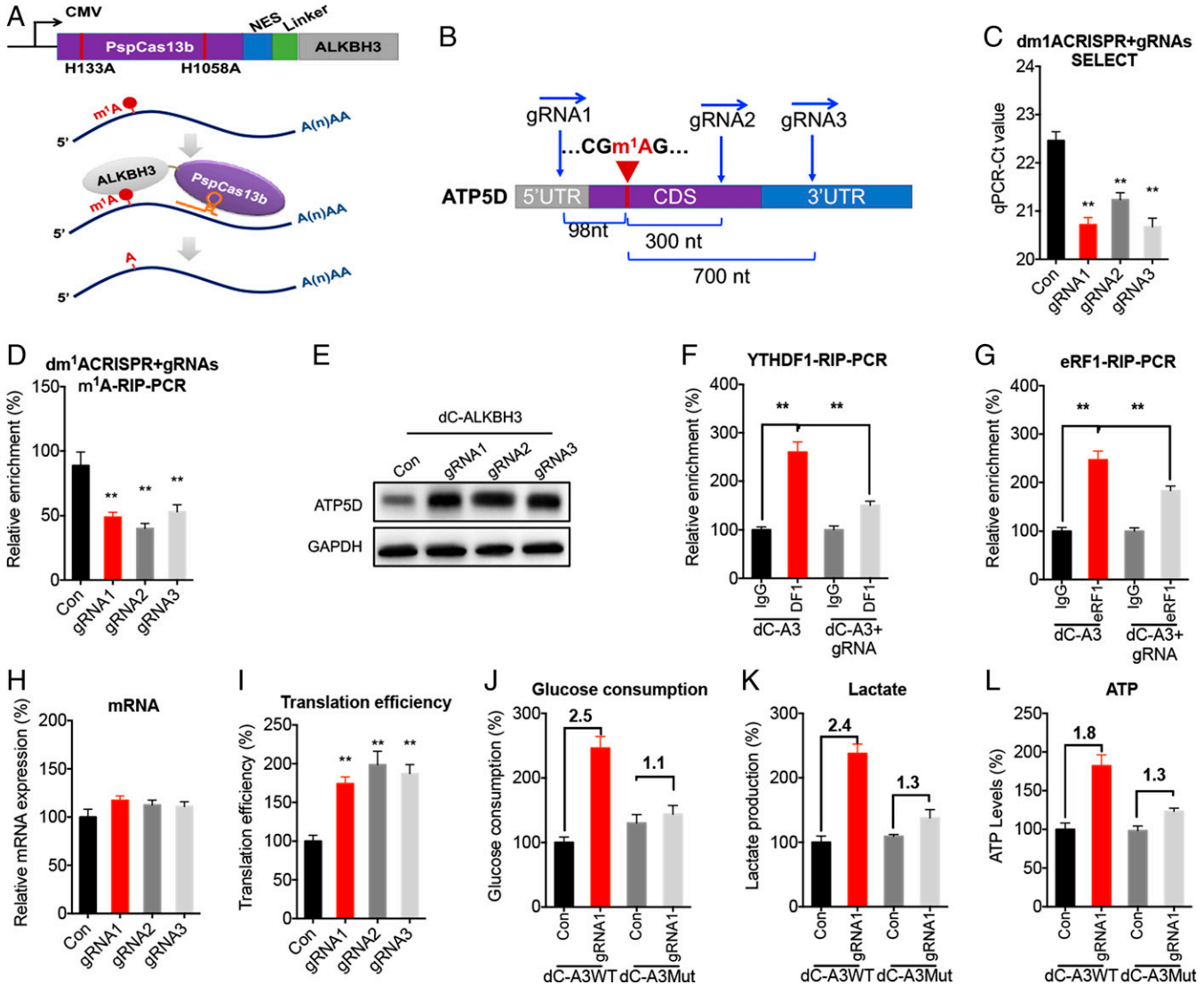

Fig. 7. Targeting m^{1}A of ATP5D by dm^{1}ACRISPR reprograms metabolic of cancer cells. (*A*) Schematic illustration of the domain organization of the dCas13b-ALKBH3 expression cassette and site-specific RNA targeting using dCas13b-guided fusion proteins. (*B*) Schematic representation of positions of m^{1}A site within *ATP5D* mRNA and the regions targeted by three gRNAs, respectively. (*C*) The C_t of qPCR showing SELECT results for detecting m^{1}A site in the potential m^{1}A site of *ATP5D*. (*D*) The C_t of qPCR showing SELECT results for detecting m^{1}A site in *ATP5D* in HeLa cells transfected with dCas13b-ALKBH3 combined with gRNA control or gRNA1/2/3, respectively, for 24 h. (*E*) The protein expression of ATP5D in HeLa cells transfected with dCas13b-ALKBH3 combined with gRNA control or gRNA1/2/3, respectively, for 24 h. (*F* and *G*) RIP-qPCR analysis of *ATP5D* mRNA in HeLa cells transfected with dCas13b-ALKBH3 combined with gRNA control (dC-A3) or gRNA for ATP5D (dC-A3 + gRNA) for 24 h by use of antibodies against YTHDF1 (*F*) and eRF1 (*G*), respectively. (*H* and *I*) The mRNA expression (*H*) and translation efficiency (*I*) of ATP5D in HeLa cells transfected with dCas13b-ALKBH3 combined with gRNA control or gRNA1/2/3, respectively, for 24 h. (*J* and *L*) The glucose consumption (*J*), lactate production (*K*), and ATP levels (*L*) in HeLa cells transfected with gRNA control, gRNA1 for *ATP5D*, and dCas13b-ALKBH5 or dCas13b-ALKBH5-Mut for 24 h.

ATP5D led to a significant up-regulation of protein expression (Fig. 7*E*), while it had limited effect on mRNA expression (*SI Appendix*, Fig. S7*E*), which was due to that the decrease of binding between *ATP5D* mRNA with YTHDF1 (Fig. 7*F*) and eRF1 (Fig. 7*G*). Further, targeted demethylation of ATP5D m^{1}A had a limited effect on mRNA levels (Fig. 7*H*), while increasing translation efficiency (Fig. 7*I*) of ATP5D mRNA, indicating that dm^{1}A-CRISPR increased translation via demethylation of m^{1}A at CDS in the case of ATP5D.

We further generated catalytically inactive dCas13b-ALKBH3 mutant (ALKBH3-R122S), which had no effect on the m^{1}A methylation of ATP5D mRNA (*SI Appendix*, Fig. S7*E*) and its protein expression (*SI Appendix*, Fig. S7*F*), whereas gRNA1 combined with dCas13b-ALKBH3 significantly increased the glucose consumption (Fig. 7*J*), lactate production (Fig. 7*K*), and ATP productions (Fig. 7*L*) as compared with that of negative gRNA. However, gRNA1 for ATP5D combined with dCas13b-ALKBH3 mutant had no significant effect on glycolysis and ATP generation (Fig. 7*J–L*). This suggests that targeting m^{1}A of ATP5D by dm^{1}ACRISPR can regulate the glycolysis and ATP generation of cancer cells.

m^{1}A/ATP5D Axis Regulated Cervical Cancer Progression. We further questioned m^{1}A/ATP5D axis on the cancer progression. Overexpression of ATP5D can reverse the suppressed growth rate of ALKBH3 KD HeLa (Fig. 8*A*) and SiHa (*SI Appendix*, Fig. S8*A*) cells and the suppression effect on migration (Fig. 8*B*) and invasion (Fig. 8*C*) of *ALKBH3*$^{-/-}$ HeLa cells, whereas mutated A71C ATP5D construct had significantly less effect than that of WT-ATP5D-reversed proliferation, migration, and invasion of *ALKBH3*$^{-/-}$ HeLa cells (Fig. 8 *A–C*). Further, HeLa WT, *ALKBH3*$^{-/-}$, WT^{ATP5D}, *ALKBH3*$^{-/-\ ATP5D}$, and *ALKBH3*$^{-/-\ ATP5D\text{-}Mut}$ stable cells were used to establish xenografts (*SI Appendix*, Fig. S8*B*). Consistently, overexpression of ATP5D can attenuate the suppression effect of *ALKBH3*$^{-/-}$ HeLa cells on in vivo tumor growth, however, this effect was markedly abolished by the mutant of A71C ATP5D (Fig. 8*D*). Immunohistochemistry (IHC) showed that ALKBH3 depletion led to a lower level of ATP5D in xenograft tumor tissues (Fig. 8*E*).

We investigated the possibility of a link between m^{1}A methylation, ATP5D, and cancer development. ALKBH3 expression in cervical cancer tissues was significantly ($P < 0.01$) greater than that in normal tissues, according to Biewenga Cervix (Fig. 8*F*) and Pyeon Multi-Cancer (Fig. 8*G*) data from the Oncomine database. Consistently, the expression of ATP5D was significantly ($P<0.01$) increased in cervical cancer tissues compared with normal tissues according to the data from Scotto Cervix (Fig. 8*H*) and Zhai Cervix (Fig. 8*I*). In addition, YTHDF1 was also increased in in cervical cancer tissues according to the data from Scotto Cervix (*SI Appendix*, Fig. S8*C*) and Biewenga Cervix (*SI Appendix*, Fig. S8*D*). The expression of ALKBH3 (Fig. 8*J*) and E2F1 (*SI Appendix*, Fig. S8*E*) was positively correlated with ATP5D in cervical cancer patients. Further, cervical cancer patients with increased expression of ALKBH3 (Fig. 8*K*) and ATP5D (Fig. 8*L*) showed reduced overall survival (OS). This suggests that the m^{1}A/ATP5D axis regulates cervical cancer progression.

Discussion

As a hallmark, cancer cells heavily rely on glycolysis to obtain energy regardless of the presence of oxygen (9). Our present study revealed that m^{1}A can regulate the translation and transcription of ATP5D, the δ subunit of ATP synthase (19), to regulate cancer cell glycolysis (Fig. 8*M*). To our knowledge, this is the first study to reveal that m^{1}A function as metabolic regulator of cancer cells, which further confirms the important roles of RNA medication on cancer cell glycolysis and metabolism.

Up to now, controversy has remained around the number and function of m1A sites in the transcriptome, possibly due to differences experimental procedures may resulting in different quality of sequencing datasets Studies have indicated that m^{1}A modifies hundreds to thousand mRNAs in human cells (2, 3, 6, 25), however, Safra et al. (5) identified only 15 m^{1}A sites in mRNAs and long non-coding RNAs (lncRNAs), with 9 in cytosolic mRNAs, 1 in cytosolic lncRNAs, and 5 in mitochondrial RNAs (mtRNAs). Here, we provide solid evidence that ATP5D was modified at A71 of exon 1 and its expression was regulated by m^{1}A modification: (1) m^{1}A-RIP-qPCR showed a significant enrichment of ATP5D mRNA, while SELECT-PCR confirmed the delay at qPCR for A71 of exon 1; (2) ALKBH3 can regulate the m^{1}A methylation and ATP5D expression via m^{1}A-related enzyme activities; (3) RT was arrested at m^{1}A-71, but not at A53 or A105 (Fig. 5*G*), indicating m^{1}A-71 is a true methylation residue (6, 30); and (4) ATP5D had been reported to be modified by m^{1}A in human cells by various previous studies (2, 3, 22, 37). Our data confirmed that the m^{1}A at A71 of the ATP5D exon 1 exists and is reversibly modified.

Little is known about biological function and roles of m^{1}A in cancers. We found that the m^{1}A of ATP5D mRNA can recruit m^{1}A reader YTHDF1, which forms a complex with eRF1, to facilitate the translation termination and decrease translation efficiency. m^{1}A at CDS in mtRNA can prevent the effective translation of modified codons due to the Watson–Crick disruptive nature (5, 6). Ribosome profiling also revealed that m^{1}A at 5′ cap and 5′ UTR in nuclear mRNA may play a role in promoting translation (6). Here, our results reveal that YTHDF1/eRF1 can bind with m^{1}A methylated mRNA to trigger mRNA release from translation machinery, which might be a mechanism which was responsible for m^{1}A suppressed mRNA translation.

We also found that m^{1}A also regulates mRNA stability of E2F1, which directly binds with ATP5D promoter to initiate its transcription. A recent study indicated that ALKBH3-induced m^{1}A demethylation increases the CSF-1 mRNA stability in breast and ovarian cancer cells to trigger cell invasion (30). Another study suggested that m^{1}A "reader" YTHDF3 bound to mRNA of IGF1R to promote mRNA degradation (25). Similarly, our data show that deletion of m^{1}A demethylase ALKBH3 can decrease the mRNA stability of E2F1. The presence of m^{1}A at different codons may lead to not only stalling of translation but also decay of the target mRNA due to mechanisms such as no-go decay with stalled ribosomes (38). Mechanisms involved in ALKBH3-regulated E2F1 mRNA stability need further investigation.

Collectively, our study sheds light on how m^{1}A methylation of RNA regulates the cell metabolic process. We cannot exclude the possibility that other genes were also involved in m^{1}A-regulated metabolic shifting—ALKBH3 demethylates m^{1}A and m^{3}C in RNA and single-stranded DNA (7)—and other factors may also contribute to ALKBH3-regulated expression of ATP5D. However, our study reveals a crosstalk of mRNA m^{1}A modification and cell metabolism, furthermore, the results expand our understanding of m^{1}A on mRNA expression and indicate the direction for therapeutic application. Our data also suggest that ALKBH3/m^{1}A/ATP5D signals may serve as useful target molecules for human cancer therapy.

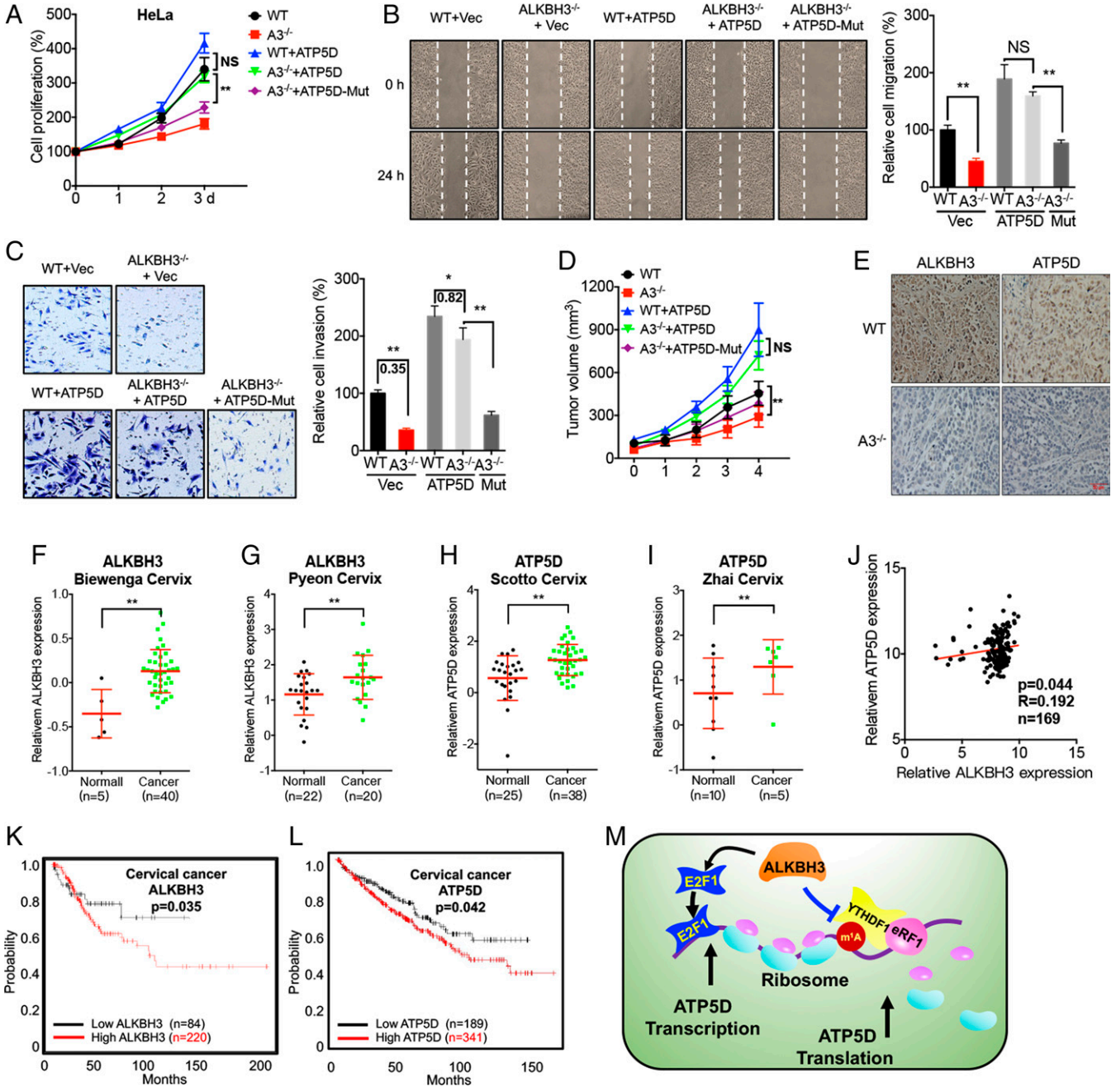

Fig. 8. m^{1}A/ATP5D axis regulated cervical cancer progression. (*A* and *C*) The relative cell proliferation (*A*), migration (*B*), and invasion (*C*) of WT and ALKBH3$^{-/-}$ HeLa cells transfected with vector control, ATP5D-WT, or ATP5D-A71C constructs. (*D*) The tumor growth curves of WT and ALKBH3$^{-/-}$ HeLa cells stably transfected with vector control, ATP5D-WT, or ATP5D-A71C constructs. (*E*) IHC (ALKBH3 and ATP5D)-stained paraffin-embedded sections obtained from WT and ALKBH3$^{-/-}$ HeLa cells. (Scale bar: 50 μM.) (*F*–*I*) The relative mRNA expression of ALKBH3 or ATP5D in Oncomine datasets. (*J*) Correlation between *ALKBH3* and *ATP5D* in cervical cancer patients (n = 169) from TCGA database. (*K* and *L*) The Kaplan-Meier survival curves of OS based on ALKBH3 (*K*) and ATP5D (*L*) expression in cervical cancer patients from TCGA database. (*M*) Proposed model to illustrate the mechanisms of m^{1}A-regulated transcription and translation of ATP5D in cancer cells.

Materials and Methods

SELECT qPCR for m^{1}A Detection. SELECT qPCR method was following Xiao's protocol (31) with slight modifications. Qubit (Thermo Fisher Scientific) with Qubit RNA HS Assay Kit (Thermo Fisher Scientific) was used to quantified total RNAs. Then, 1,500 ng of total RNA was mixed with 40 nM up and down primers and 5 μM dNTP in 17 μL 1× CutSmart buffer (NEB). The mixture was incubated with the follow program: 90 °C for 1 min, 80 °C for 1 min, 70 °C for 1 min, 60 °C for 1 min, 50 °C for 1 min, and 40 °C for 6 min. The sample was further mixed with 0.5 U SplintR ligase, 10 nM ATP, and 3 μL of 0.01 U Bst 2.0 DNA polymerase and incubated at 40 °C for 20 min and denatured at 80 °C for 20 min. After, 20 μL qPCR reaction containing 2 μL of final reaction mixture, 2× SYBR Green Master Mix (TaKaRa), and 200 nM SELECT primers (listed in the *SI Appendix*) was performed. The qPCR program was 95 °C, 5 min; (95 °C, 10 s; 60 °C, 35 s) × 40 cycles; 95 °C, 15 s; 60 °C, 1 min; 95 °C, 15 s; 4 °C, hold. Results were calculated by normalized the threshold cycle (C_t) values of samples to their corresponding C_t values of control. All assays were performed with three independent experiments.

Design of the Guide RNAs for dm^{1}ACRISPR. mRNA sequences of all isoforms of target genes were subjected to alignment analysis to identify the common regions, which were acted as targeting candidates for gRNA design. gRNAs targeting CDS region of ATP5D were designed, all designed gRNAs were subject to MEGABLAST (https://blast.ncbi.nlm.nih.gov/Blast.cgi) to avoid mismatching to unexpected mRNA in human genome. The sequences of gRNAs were: gRNA1, 5′-AGA ATG TTG GCG AGT CTC AC-3′; gRNA2, 5′-GGA

TCA ATG CTT CCA ATG TGG CTT GGG TTT CC-3′; and gRNA3, 5′-CAG TTA GGA TCA ATG CTT CCA ATG TGG CTT GG-3′.

Database Analysis. ATP5D and ALKBH3 expression in cervical cancer from Oncomine database (Zhai Cervix, Biewenga Cervical, Scotto Cervical, and Pyeon Multiple Cancer) was analyzed. The correlation between ATP5D and ALKBH3 was evaluated by use of LinkedOmics (http://www.linkedomics.orglogin.php.), which is a publicly available portal that includes multiomics data from all 32 cancer types from The Cancer Genome Atlas (TCGA) (39). Kaplan-Meier plotter (http://kmplot.com/analysis/) (40) was used to assess the prognostic value of ALKBH3, ATP5D, E2F1, YTHDF1, and eRF1 expression in patients with cervical cancers.

Statistical Analyses. Data were reported as mean ± SD from at least three independent experiments. For statistical analysis, two-tailed unpaired Student's *t* test between two groups and by one-way or two-way ANOVA followed by Bonferroni test for multiple comparison were performed. All statistical tests were two-sided. Data analysis was carried out using SPSS 16.0 for Windows. A *P* value of <0.05 was considered to be statistically significant. $*P < 0.05$, $**P < 0.01$; NS, no significant.

The other methods are reported in the *SI Appendix* due to the length restrictions.

Data Availability. The accession number for the high-throughput of mRNA-seq data reported in this paper is SRP: SRP277280 (https://www.ncbi.nlm.nih.gov/sra/?term=SRP277280) (41). The accession number for the high-throughput of m^{1}A-seq and Ribo-seq data reported in this paper is GEO: GSE195637 (https://www.ncbi.nlm.nih.gov/geo/query/acc.cgi?acc=GSE195637) (42) and GSE195703 (https://www.ncbi.nlm.nih.gov/geo/query/acc.cgi?acc=GSE195703) (43). The data underlying Fig. 8 *F–O* referenced during the study are available in a public repository from The Cancer Genome Atlas website. All the other data supporting the findings of this study are included in the article and/or *SI Appendix*.

ACKNOWLEDGMENTS. We thank Professor Chengqi Yi at Peking University for experimental skills and instrumental help. This research was supported by the National Natural Science Foundation of China (32161143017, 82173833, 82103296, 82173126, 81973343, and 82072559), The International Cooperation Project of the Science and Technology Planning Project of Guangdong Province, China (2021A0505030029), the Open Program of Shenzhen Bay Laboratory (SZBL202009051006), the Guangdong Provincial Key Laboratory of Chiral Molecule and Drug Discovery (2019B030301005), and the Guangdong Basic and Applied Basic Research Foundation (2020A1515010291).

Author affiliations: [a]Guangdong Provincial Key Laboratory of New Drug Design and Evaluation, School of Pharmaceutical Sciences, Sun Yat-sen University, Guangzhou 510006, China; [b]Transformation Engineering Research Center of Chronic Disease Diagnosis and Treatment, Department of Physiology, School of Basic Medicine, Guizhou Medical University, Guiyang 550025, China; [c]Sun Yat-sen University Cancer Center, State Key Laboratory of Oncology in South China; Collaborative Innovation Center for Cancer Medicine, Guangzhou 510060, China; and [d]Department of General Practice, Zhujiang Hospital, Southern Medical University, Guangzhou, China

1. D. B. Dunn, The occurrence of 1-methyladenine in ribonucleic acid. *Biochim. Biophys. Acta* **46**, 198–200 (1961).
2. D. Dominissini *et al.*, The dynamic N(1)-methyladenosine methylome in eukaryotic messenger RNA. *Nature* **530**, 441–446 (2016).
3. X. Li *et al.*, Transcriptome-wide mapping reveals reversible and dynamic N(1)-methyladenosine methylome. *Nat. Chem. Biol.* **12**, 311–316 (2016).
4. H. Zhou *et al.*, m(1)A and m(1)G disrupt A-RNA structure through the intrinsic instability of Hoogsteen base pairs. *Nat. Struct. Mol. Biol.* **23**, 803–810 (2016).
5. M. Safra *et al.*, The m1A landscape on cytosolic and mitochondrial mRNA at single-base resolution. *Nature* **551**, 251–255 (2017).
6. X. Li *et al.*, Base-resolution mapping reveals distinct m^{1}A methylome in nuclear- and mitochondrial-encoded transcripts. *Mol. Cell* **68**, 993–1005.e9 (2017).
7. P. A. Aas *et al.*, Human and bacterial oxidative demethylases repair alkylation damage in both RNA and DNA. *Nature* **421**, 859–863 (2003).
8. D. Hanahan, R. A. Weinberg, Hallmarks of cancer: The next generation. *Cell* **144**, 646–674 (2011).
9. O. Warburg, On the origin of cancer cells. *Science* **123**, 309–314 (1956).
10. N. N. Pavlova, C. B. Thompson, The emerging hallmarks of cancer metabolism. *Cell Metab.* **23**, 27–47 (2016).
11. A. R. Cantelmo *et al.*, Inhibition of the glycolytic activator PFKFB3 in endothelium induces tumor vessel normalization, impairs metastasis, and improves chemotherapy. *Cancer Cell* **30**, 968–985 (2016).
12. E. Zhao *et al.*, Cancer mediates effector T cell dysfunction by targeting microRNAs and EZH2 via glycolysis restriction. *Nat. Immunol.* **17**, 95–103 (2016).
13. H. Wang, Y. Yang, J. Liu, L. Qian, Direct cell reprogramming: Approaches, mechanisms and progress. *Nat. Rev. Mol. Cell Biol.* **22**, 410–424 (2021).
14. F. Kottakis *et al.*, LKB1 loss links serine metabolism to DNA methylation and tumorigenesis. *Nature* **539**, 390–395 (2016).
15. D. Zhang *et al.*, Metabolic regulation of gene expression by histone lactylation. *Nature* **574**, 575–580 (2019).
16. B. Zhou *et al.*, N(6) -methyladenosine reader protein YT521-B homology domain-containing 2 suppresses liver steatosis by regulation of mRNA stability of lipogenic genes. *Hepatology* **73**, 91–103 (2020).
17. Y. Qing *et al.*, R-2-hydroxyglutarate attenuates aerobic glycolysis in leukemia by targeting the FTO/m^{6}A/PFKP/LDHB axis. *Mol. Cell* **81**, 922–939.e9 (2021).
18. Z. Li *et al.*, N^6-methyladenosine regulates glycolysis of cancer cells through PDK4. *Nat. Commun.* **11**, 2578 (2020).
19. C. von Ballmoos, A. Wiedenmann, P. Dimroth, Essentials for ATP synthesis by F1F0 ATP synthases. *Annu. Rev. Biochem.* **78**, 649–672 (2009).
20. Z. Chen *et al.*, Transfer RNA demethylase ALKBH3 promotes cancer progression via induction of tRNA-derived small RNAs. *Nucleic Acids Res.* **47**, 2533–2545 (2019).
21. A. V. Grozhik *et al.*, Antibody cross-reactivity accounts for widespread appearance of m^{1}A in 5'UTRs. *Nat. Commun.* **10**, 5126 (2019).
22. R. Esteve-Puig *et al.*, Epigenetic loss of m1A RNA demethylase ALKBH3 in Hodgkin lymphoma targets collagen, conferring poor clinical outcome. *Blood* **137**, 994–999 (2021).
23. M. Oláhová *et al.*; Undiagnosed Diseases Network, Biallelic mutations in ATP5F1D, which encodes a subunit of ATP synthase, cause a metabolic disorder. *Am. J. Hum. Genet.* **102**, 494–504 (2018).
24. X. Wang *et al.*, N(6)-methyladenosine modulates messenger RNA translation efficiency. *Cell* **161**, 1388–1399 (2015).
25. Q. Zheng *et al.*, Cytoplasmic m^{1}A reader YTHDF3 inhibits trophoblast invasion by downregulation of m^{1}A-methylated IGF1R. *Cell Discov.* **6**, 12 (2020).
26. X. Dai, T. Wang, G. Gonzalez, Y. Wang, Identification of YTH domain-containing proteins as the readers for N^1-methyladenosine in RNA. *Anal. Chem.* **90**, 6380–6384 (2018).
27. K. W. Seo, R. E. Kleiner, YTHDF2 recognition of N^1-methyladenosine (m^{1}A)-modified RNA is associated with transcript destabilization. *ACS Chem. Biol.* **15**, 132–139 (2020).
28. C. Beißel *et al.*, Translation termination depends on the sequential ribosomal entry of eRF1 and eRF3. *Nucleic Acids Res.* **47**, 4798–4813 (2019).
29. K. D. Meyer *et al.*, 5′ UTR m(6)A promotes cap-independent translation. *Cell* **163**, 999–1010 (2015).
30. H. H. Woo, S. K. Chambers, Human ALKBH3-induced m^{1}A demethylation increases the CSF-1 mRNA stability in breast and ovarian cancer cells. *Biochim. Biophys. Acta. Gene Regul. Mech.* **1862**, 35–46 (2019).
31. Y. Xiao *et al.*, An elongation- and ligation-based qPCR amplification method for the radiolabeling-free detection of locus-specific N^6 -methyladenosine modification. *Angew. Chem. Int. Ed. Engl.* **57**, 15995–16000 (2018).
32. K. R. Zhou *et al.*, ChIPBase v2.0: Decoding transcriptional regulatory networks of non-coding RNAs and protein-coding genes from ChIP-seq data. *Nucleic Acids Res.* **45** (D1), D43–D50 (2017).
33. A. Khan, A. Mathelier, JASPAR RESTful API: Accessing JASPAR data from any programming language. *Bioinformatics* **34**, 1612–1614 (2018).
34. J. A. Castro-Mondragon *et al.*, JASPAR 2022: The 9th release of the open-access database of transcription factor binding profiles. *Nucleic Acids Res.* **50** (D1), D165–D173 (2022).
35. X. Wang *et al.*, N^6-methyladenosine-dependent regulation of messenger RNA stability. *Nature* **505**, 117–120 (2014).
36. J. Li *et al.*, Targeted mRNA demethylation using an engineered dCas13b-ALKBH5 fusion protein. *Nucleic Acids Res.* **48**, 5684–5694 (2020).
37. H. Zhou *et al.*, Evolution of a reverse transcriptase to map N^1-methyladenosine in human messenger RNA. *Nat. Methods* **16**, 1281–1288 (2019).
38. K. Ikeuchi, T. Izawa, T. Inada, Recent progress on the molecular mechanism of quality controls induced by ribosome stalling. *Front. Genet.* **9**, 743 (2019).
39. S. V. Vasaikar, P. Straub, J. Wang, B. Zhang, LinkedOmics: Analyzing multi-omics data within and across 32 cancer types. *Nucleic Acids Res.* **46** (D1), D956–D963 (2018).
40. B. Győrffy, P. Surowiak, J. Budczies, A. Lánczky, Online survival analysis software to assess the prognostic value of biomarkers using transcriptomic data in non-small-cell lung cancer. *PLoS One* **8**, e82241 (2013).
41. Y. Wu *et al.*, RNA m^{1}A methylation regulates glycolysis of cancer cells through modulating ATP5D. SRP: SRP277280. https://www.ncbi.nlm.nih.gov/sra/?term=SRP277280. Deposited 28 January 2022.
42. Y. Wu *et al.*, RNA m^{1}A methylation regulates glycolysis of cancer cells through modulating ATP5D. GEO: GSE195637. https://www.ncbi.nlm.nih.gov/geo/query/acc.cgi?acc=GSE195637. Deposited 28 January 2022.
43. Y. Wu *et al.*, RNA m^{1}A methylation regulates glycolysis of cancer cells through modulating ATP5D. GEO: GSE195703. https://www.ncbi.nlm.nih.gov/geo/query/acc.cgi?acc=GSE195703. Deposited 28 January 2022.